Inorg. Chem. **2006**, *45*, 5739–5741

Electrical Conductivity Modulation Coupled to a High-Spin–Low-Spin Conversion in the Molecular System $[Fe^{III}(qsal)_2][Ni(dmit)_2]_3 \cdot CH_3CN \cdot H_2O$

Kazuyuki Takahashi,*,† Heng-Bo Cui,† Yoshinori Okano,† Hayao Kobayashi,*,† Yasuaki Einaga,‡ and Osamu Sato§

Institute for Molecular Science and CREST, JST, Okazaki 444-8585, Japan, Department of Chemistry, Keio University, Yokohama 223-8522, Japan, and Institute for Materials Chemistry and Engineering, Kyushu University Fukuoka 816-8508, Japan

Received May 17, 2006

The synergy between the electrical conductivity within the stacks of $Ni(dmit)_2$ in the newly electrocrystallized $[Fe(qsal)_2][Ni(dmit)_2]_3 \cdot CH_3CN \cdot H_2O$ and the spin conversion of $Fe(qsal)_2$ is evidenced. In addition, the presence of a light-induced excited spin state trapping effect suggests that this complex is a prototypal photoswitchable spin-crossover molecular conductor.

Recently considerable interest has been devoted to the development of molecular conducting materials exhibiting the synergy between conductivity and magnetism. Along this line, a paramagnetic superconductor,[1] a ferromagnetic metal,[2] and an antiferromagnetic superconductor[3] have been developed. In particular, the discovery of the field-induced superconducting transition in λ-$(BETS)_2FeCl_4$[4] gave a splendid example of the synergetic action of conduction electrons and localized magnetic moments in the hybrid system.

As another kind of correlation between electrical conductivity and magnetism, the conducting state switching driven by a temperature-induced charge transfer was reported in an Fe mixed-valence complex[5] and Prussian blue analogues.[6] Although these switching phenomena are very attractive, it has been difficult to develop other molecular conducting system by using related molecular magnetic materials because these systems are almost in the insulating states and their conduction mechanisms are not clear. On the other hand, it is well known that the electrical properties of molecular conductors are very sensitive to small modifications of their crystal structures. This means that it can be controlled by a structural change. Thus, we have focused our attention on combining mixed-valency in organics or metal−organic systems with spin-crossover (SCO) components because the spin transition (low-spin (LS)—high-spin (HS)) is accompanied by considerable changes in coordination bond lengths and geometries.[7] Furthermore, given that the spin transition can be controlled by external perturbations, such as temperature, pressure, and light, it would be possible to control the electrical conductivity of an SCO−molecular conductor reversibly. Consequently, we have developed Fe(II) and Fe(III) SCO complexes with redox-active components based on 1,3-dithiol-2-ylidene[8] and $Ni(dmit)_2$[9] [dmit = 4,5-dithiolato-1,3-dithiole-2-thione], respectively. These have the potential electrical conducting properties. Both complexes showed spin transitions and light-induced excited spin state trapping (LIESST) effects, suggesting that they are promising candidates for photocontrollable SCO molecular conductors. As a similar approach to SCO conducting complexes, a TCNQ anion radical salt[10] and a $Ni(dmit)_2$ salt[11] involving the Fe(III) SCO ion as a countercation are known [TCNQ = 7,7,8,8-tetracyanoquinodimethane]. However, the direct synergy between electrical conductivity and spin conversion has never been evidenced. In this paper, we describe the clear observation of the coupling between the electrical properties and the spin transition in the SCO molecular conductor, [Fe-

* To whom correspondence should be addressed. E-mail: ktaka@ims.ac.jp.
† Institute for Molecular Science and CREST, JST.
‡ Keio University.
§ Kyushu University.

(1) Kurmoo, M.; Graham, A. W.; Day, P.; Coles, S. J.; Hursthouse, M. B.; Caulfield J. L.; Singleton J.; Pratt F. L.; Hayes W.; Ducasse L.; Guionneau, P. *J. Am. Chem. Soc.* **1995**, *117*, 12209.
(2) Coronado, E.; Galán-Mascarós, J. R.; Gómez-García, C. J.; Laukhin, V. *Nature* **2000**, *408*, 447.
(3) Ojima, E.; Fujiwara, H.; Kato, K.; Kobayashi, H.; Tanaka, H.; Kobayashi, A.; Tokumoto, M.; Cassoux, P. *J. Am. Chem.* Soc. **1999**, *121*, 5581. Fujiwara, H.; Fujiwara, E.; Nakazawa, Y.; Narymbetov, B. Z.; Kato, K.; Kobayashi, H.; Kobayashi, A.; Tokumoto, M.; Cassoux, P. *J. Am. Chem. Soc.* **2001**, *123*, 306.
(4) Uji, S.; Shinagawa, H.; Terashima, T.; Yakabe, T.; Terai, Y.; Tokumoto, M.; Kobayashi, A.; Tanaka, H.; Kobayashi, H. *Nature* **2001**, *410*, 908.
(5) Enomoto, M.; Itoi, M.; Ono, Y.; Okubo, M.; Kojima, N. *Synth. Met.* **2003**, *137*, 1231.
(6) Sato, O.; Kawakami, T.; Kimura, M.; Hishiya, S.; Kubo, S.; Einaga, Y. *J. Am. Chem. Soc.* **2004**, *126*, 13176.
(7) Marchive, M.; Guionneau, P.; Howard, J. A. K.; Chastanet, G.; Létard, J.-F.; Goeta, A. E.; Chasseau, D. *J. Am. Chem.* Soc. **2002**, *124*, 194.
(8) Takahashi, K.; Kawakami, T.; Gu, Z.-Z.; Einaga, Y.; Fujishima, A.; Sato, O. *Chem. Commun.* **2003**, 2374.
(9) Takahashi, K.; Cui, H.-B.; Kobayashi, H.; Einaga, Y.; Sato, O. *Chem. Lett.* **2005**, *34*, 1240.
(10) Nakano, M.; Fujita, N.; Matsubayashi, G.; Mori, W. *Mol. Cryst. Liq. Cryst.* **2002**, *379*, 365.
(11) Dorbes, S.; Valade, L.; Real, J. A.; Faulmann, C. *Chem. Commun.* **2005**, 69.

10.1021/ic060852l CCC: $33.50
Published on Web 06/21/2006

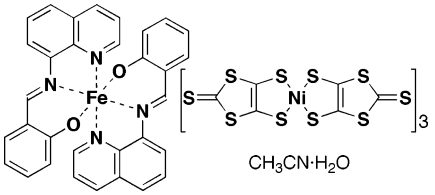

Figure 1. Molecular structure of $[Fe(qsal)_2][Ni(dmit)_2]\cdot CH_3CN\cdot H_2O$.

$(qsal)_2][Ni(dmit)_2]_3\cdot CH_3CN\cdot H_2O$ [qsalH = *N*-(8-quinolyl)-salicylaldimine]. The LIESST effect on this complex is also presented.

The complex was prepared by applying a constant voltage (1.5 V) to the dry acetonitrile solution of $[Fe(qsal)_2][Ni(dmit)_2]\cdot 2CH_3CN$[9] in an H-type glass cell with Pt electrodes. The crystals grew on the anode as very thin dark brown platelets. The EDX analyses indicate that the ratio of Fe to Ni is 1:3 for all the crystals examined. This complex is, hereafter, designated as the 1:3 complex. Its crystal structure was determined at room temperature (Figure 2),[12] though most crystals were heavily twinned. There are two $Fe(qsal)_2$ and six $Ni(dmit)_2$ crystallographically independent molecules in the unit cell. The numbers of solvent molecules found by the difference Fourier map were decided by convergence of the least-squares refinement cycle. $Ni(dmit)_2$ molecules are arranged in a face-to-face manner to form a 6-fold column along the *b* axis. These columns are arranged in a herringbone-type side-by-side manner to generate layers along the transverse direction. The overlap integrals based on extended Hückel calculations indicate that $Ni(dmit)_2$ molecules formed a trimer within a column and there was no favorable exchange interaction between columns. $Fe(qsal)_2$ cations are dimerized by $\pi-\pi$ interactions. The $Fe(qsal)_2$ dimers construct a one-dimensional chain parallel to the Fe−Fe direction of a dimer,[9] which is the $a + b$ direction in the present case. Thus, $Fe(qsal)_2$ chains were interwoven with the $Ni(dmit)_2$ columns.

Temperature dependence of the electrical resistivity of a single crystal was measured by a HUSO HECS 9065 conductometer using a conventional four-probe method in the temperature range of 70−300 K (Figure 3). Though the crystal showed semiconducting behavior, the room-temperature conductivity was relatively high ($\sigma_{RT} = 2.0$ S cm^{-1}). Interestingly, a hysteretic behavior in the resistivity was observed in the temperature range of 90−120 K. Note that the resistivity in the heating process was lower than that in the cooling process, which is contrary to the hysteretic behaviors observed in molecular conductors. The activation energy in the low-temperature phase ($E_a = 0.17$ eV between 70 and 90 K) was lower than that in the high-temperature phase ($E_a = 0.25$ eV between 125 and 250 K).

Temperature dependence of the magnetic susceptibility of the sample consisting of only crystals on the anode was measured by a Quantum Design MPMS-XL SQUID magnetometer in the temperature range of 2−300 K (Figure 4). The value of $\chi_M T$ at 300 K is 3.75 emu K mol^{-1}, suggesting the coexistence of 84% of the Fe(III) HS state and 16% of the LS state. The HS ratio was consistent with that estimated

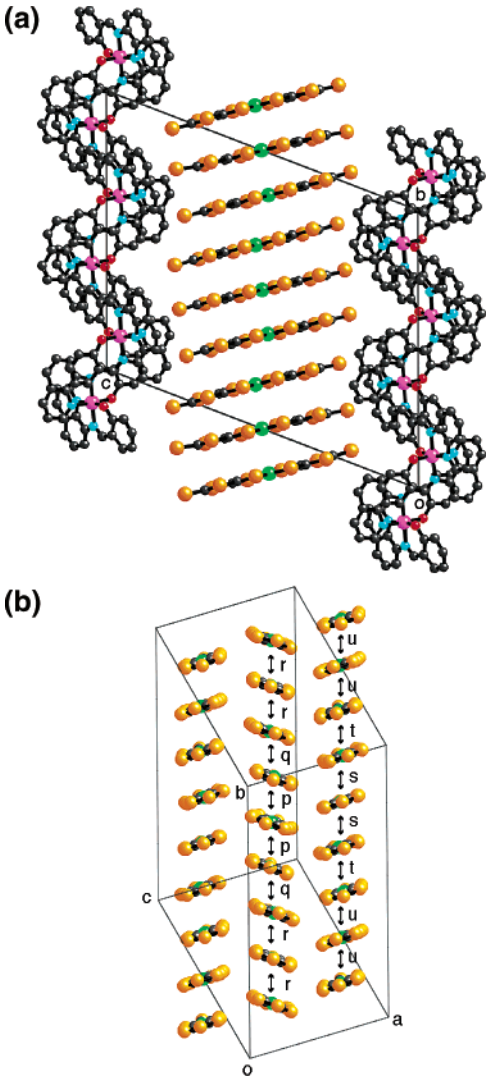

Figure 2. Crystal structures of $[Fe(qsal)_2][Ni(dmit)_2]_3\cdot CH_3CN\cdot H_2O$. (a) Viewed along the *a* axis. The solvent molecules were omitted for clarity. (b) End-on projection of one $Ni(dmit)_2$ layer. The overlap integrals of the LUMO of $Ni(dmit)_2$ are $p = -13.7$, $q = -5.27$, $r = 11.9$, $s = -10.8$, $t = -3.24$, and $u = -11.1 \times 10^{-3}$, respectively. The overlap integrals between columns are below 0.6×10^{-3}.

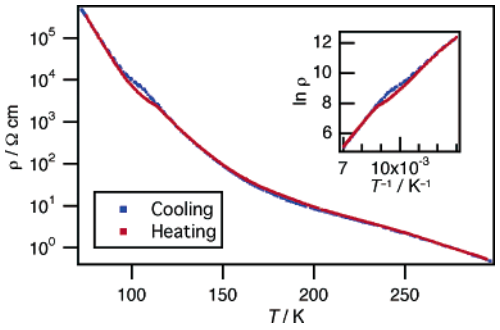

Figure 3. Temperature dependence of the resistivity of a single crystal of $[Fe(qsal)_2][Ni(dmit)_2]_3\cdot CH_3CN\cdot H_2O$. The inset shows the Arrhenius plot of the 1:3 complex.

(12) X-ray data for the 1:3 complex: triclinic, $P\bar{1}$ (No.2), $a = 12.5203(5)$ Å, $b = 22.94040(10)$ Å, $c = 26.8278(5)$ Å, $\alpha = 68.242(7)°$, $\beta = 84.900(8)°$, $\gamma = 76.956(8)°$, $V = 6971.8(3)$ Å^3, $Z = 4$, $D_{calcd} = 1.871$ g cm^{-3}, R1 = 0.062 ($I > 3\sigma(I)$), wR2 = 0.091 ($I > 3\sigma(I)$), GOF = 1.002. The Ni, Fe, and S atoms were refined anisotropically, and the rest of the non-hydrogen atoms except solvent molecules were refined isotropically.

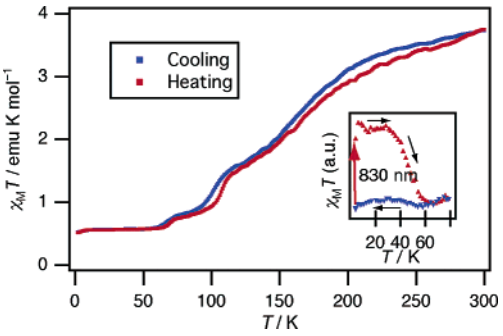

Figure 4. $\chi_M T$ vs T plot of $[Fe(qsal)_2][Ni(dmit)_2]_3 \cdot CH_3CN \cdot H_2O$. The sweep speed is 1 K min^{-1}. The inset shows the LIESST effect of the 1:3 complex.

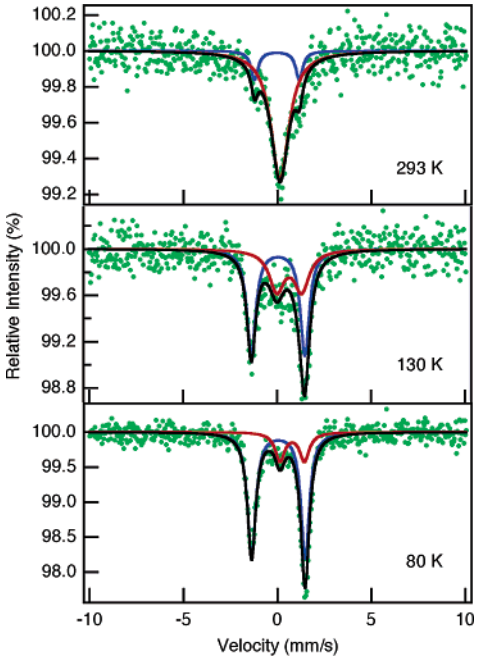

Figure 5. Temperature dependence of Mössbauer spectra of $[^{57}Fe(qsal)_2][Ni(dmit)_2]_3 \cdot CH_3CN \cdot H_2O$. Green dots, observed spectra; blue line, simulated LS curve; red line, simulated HS curve; black line, the sum of the simulated LS and HS curves. Mössbauer Parameters; 293 K: HS (85.0%) I.S. = 0.139, Q.S. = 0, LS (15.0%) I.S. = −0.024, Q.S. = 2.377; 130 K: HS (39.4%) I.S. = 0.65, Q.S. = 1.32, LS (60.6%) I.S. = 0.06, Q.S. = 2.85; 80 K: HS (20.0%) I.S. = 0.79, Q.S. = 1.30, LS (80.0%) I.S. = 0.06, Q.S. = 2.85.

by Mössbauer spectroscopy of the ^{57}Fe-enriched sample at 300 K (Figure 5), which also indicated that the valence of the Fe atom is trivalent and the moment on the $Ni(dmit)_2$ stacks is negligible. On cooling, the $\chi_M T$ value gradually decreased down to 120 K and then showed a relatively abrupt two-step change. The $\chi_M T$ value below 60 K is 0.57 emu K mol^{-1}, indicating that the 1:3 complex was almost in the LS state. For the heating process, the reverse transitions appeared in each step. It should be noted that the narrow hysteresis loop between 90 and 120 K corresponds exactly to the temperature range where the anomaly in conducting behavior was observed. The HS ratios of 12% and 33% at 80 and 130 K, respectively, calculated from magnetic measurement are in good agreement with those estimated from Mössbauer spectroscopy (Figure 5). Thus, this $\chi_M T$ change is considered to be derived from the cooperative spin transition of the Fe(III) cations. The relatively low resistivity in the heating process may be due to a sort of "chemical pressure effect" associated with the spin transition. Since the smaller size of SCO ions in the LS state than in the HS state will produce the more compact molecular packing of the cationic layers, this contraction exerts a pressure to the $Ni(dmit)_2$ conducting layers to make the system more conducting. Thus, to the best of our knowledge, this is the first evidence of a resistivity anomaly coupled with a spin transition in the SCO−molecular conductor hybrid.

A preliminary LIESST experiment was carried out on the 1:3 complex (Figure 4, inset). On illuminating with a diode laser (830 nm) at 5 K, an increase in the magnetization was observed, suggesting the metastable HS state can be trapped in the 1:3 complex. This metastable state was relaxed to the ground LS state at about 60 K. This behavior is consistent with that of the metastable HS state in $[Fe(qsal)_2][Ni(dmit)_2] \cdot 2CH_3CN$.[9] We believe that if a system exhibiting a higher relaxation temperature from the metastable HS state can be designed, the photocontrollable molecular conductor will be realized. The 1:3 complex should be a precursor of such a molecular conductor.

In summary, we have observed a clear synergy between the SCO phenomenon and an electrical conduction a SCO−molecular conductor hybrid, which also displayed the LIESST effect. Thus, the 1:3 complex can be classified as a prototypal photoswitchable SCO molecular conductor. It might be possible that larger response such as the metal-to-insulator transition will be realized by external perturbations if a molecular "metal" with a suitable SCO counterion is prepared. Further trials to enhance the conductivity and to increase the relaxation temperature are now in progress.

Acknowledgment. The authors are indebted to Dr. M. Kurmoo for fruitful discussions on this work. This work was supported by CREST (Core Research for Evolutional Science and Technology).

Supporting Information Available: X-ray crystallographic information of the 1:3 complex as a CIF file. This material is available free of charge via the Internet at http://pubs.acs.org.

IC060852L